Modelling the flow within forests: the canopy-related terms in the Reynolds-averaged formulation

J. M. Viana Parente Lopes[1]**, J. M. L. M. Palma**[2],†** and A. Silva Lopes**[2]

[1]Centro de Física das Universidades do Minho e Porto, Departamento de Física e Astronomia, Faculdade de Ciências da Universidade do Porto, 4169-007 Porto, Portugal

[2]Faculdade de Engenharia da Universidade do Porto, Departamento de Engenharia Mecânica, Rua Dr Roberto Frias s/n, 4200-465 Porto, Portugal

The canopy-related terms in the transport equations for momentum, Reynolds stresses, turbulent kinetic energy and its dissipation rate were described by a perturbative expansion around a velocity scale based on the mean total kinetic energy. The quality of the series and the relative magnitude of the first orders were analysed through comparison with the results of large-eddy simulation of three canopy flows representative of real-life applications. The flows in question were those over a horizontally homogeneous forest, a sequence of forest stands and clearings, and a forested hill. The analysis gave both the highest order required for an accurate evaluation of the canopy effects and a mathematical formulation for the canopy-related terms in a Reynolds-averaged Navier–Stokes formulation. This offers a sounder basis and assured consistency for the turbulence modelling of canopy flows between Reynolds-averaged Navier–Stokes and large-eddy simulation frameworks.

Key words: atmospheric flows, turbulence modelling

1. Introduction

A forest is defined as an area of more than 0.5 ha, of which over 10 % is covered with trees with a minimum height of 5 m. Still according to the Global Forest Resource Assessment (FAO 2012, 2016), forests cover 30.6 % of Earth's total land area and their biomass and soils store more carbon than the atmosphere (Pan *et al.* 2013). It is not surprising, therefore, that the flow within forests has been a subject of research, and the review papers by Raupach & Thom (1981), Finnigan (2000), Belcher, Harman & Finnigan (2012) and Brunet (2020) offer an overview of how our understanding and modelling of forest flows have developed.

Initial studies (cf. Raupach, Thom & Edwards 1980) considered a forest to be a perturbation to the upstream boundary layer. This approach (based on the characteristic roughness, z_0, and displacement height, d) can only be successfully applied to the mean

† Email address for correspondence: jpalma@fe.up.pt

flow over large homogeneously forested regions and is most useful under conditions of insufficient spatial resolution (e.g. Silva Lopes, Palma & Piomelli 2015). Nowadays, the flow over a forest is viewed as an analogue of a mixing layer (cf. Finnigan 2000), composed of large turbulent structures that gradient-diffusion-based approaches cannot mimic. Within the forest, the flow between the complex network of trunks and leaves increases shear and, consequently, turbulence – wake production – while, at the same time, large eddies are broken into smaller ones, increasing dissipation – spectral shortcut (e.g. Novak *et al.* 2000; Cava & Katul 2008).

In the case of a higher resolution, trees are seen as a drag force (f_i), and modelled via additional contributions to the transport equations for momentum (U_i, (1.1)), turbulent kinetic energy (TKE; k, (1.2)) and its dissipation rate (ε, (1.3)). Traditionally, the canopy models in the Reynolds-averaged Navier–Stokes (RANS) formulation have the general form

$$\mathcal{F}_{U_i}^{k-\varepsilon} = -C_d a(z)|\boldsymbol{U}|U_i, \tag{1.1}$$

$$\mathcal{F}_k^{k-\varepsilon} = C_d a(z)\left(\beta_p|\boldsymbol{U}|^3 - \beta_d|\boldsymbol{U}|k\right), \tag{1.2}$$

$$\mathcal{F}_\varepsilon^{k-\varepsilon} = C_d\, a(z)\left(C_{\varepsilon 4}\beta_p|\boldsymbol{U}|^3\frac{\varepsilon}{k} - C_{\varepsilon 5}\beta_d|\boldsymbol{U}|\varepsilon\right). \tag{1.3}$$

Here C_d is a mean drag coefficient, $a(z)$ is the leaf area density (*LAD*), a function of the distance to the ground, and $|\boldsymbol{U}|$ is the mean scalar velocity, $(U_iU_i)^{1/2}$. Here, we are assuming the mathematical formulation of canopy flows in the context of the two-equation (k–ε) RANS model, first presented by Svensson & Häggkvist (1990) and Green (1992). Since this model is based on the eddy-viscosity concept, its accuracy, when compared with Reynolds-stress models, is questionable in strongly advective conditions. However, it is successfully used in the study of atmospheric flows and by the wind industry (e.g. Costa *et al.* 2006; Dalpé & Masson 2008; Abiven, Palma & Brady 2011).

Equations (1.2) and (1.3) were obtained using dimensional relations and the coefficients determined as usual in turbulence modelling; i.e. on the basis of canonical flows, with comparison of the computational and experimental results of mean wind speed, shear stress or TKE (see, for instance, Wilson 1988; Lien & Yee 2004; Lien, Yee & Wilson 2005; Sanz & Katul 2007; Sogachev *et al.* 2012) or of large-eddy simulations (LES) (Silva Lopes *et al.* 2013). Experimental data within real forests are scarce, and many of the constants have been fine-tuned with measurements taken outside forests, where the impact of such a different model (or set of constants) is lower. These equations try to accommodate the two opposing and competing phenomena of wake production and spectral shortcut. This effort, eloquently summarized in table 1, has led us to the current position, in which, in the context of two-equation turbulence modelling, neither standard parametrization nor standard values for the coefficients are available when modelling the flow over forests. Sanz (2003), Sogachev & Panferov (2006), Sanz & Katul (2007), Sogachev (2009) and Sogachev *et al.* (2012) provide some of the most comprehensive derivations of the coefficients, based on such phenomenological arguments as assuming the Kolmogorov relation, a dense and homogeneous canopy and constant mixing length within the canopy. Nevertheless, these physical constraints are insufficient and the coefficient values are found to be bound to such additional *ad hoc* restrictions as $C_{\varepsilon 4} = C_{\varepsilon 5}$ (Sanz 2003).

The forest flow parametrizations in the LES and RANS frameworks are highly similar. Both require a canopy-related term in the momentum equation and in the TKE (e) of the subgrid scales (cf. Sagaut 2006), if such an equation (1.4) is required (e.g. Shaw &

One-equation model	β_p	β_d		
Wilson, Finnigan & Raupach (1998)	—	1.0, 2.5		
Pinard & Wilson (2001)[a]	—	1.0		
Sogachev et al. (2002)	1.0	4.0		

Two-equation (k–ε) model	β_p	β_d	$C_{\varepsilon 4}$	$C_{\varepsilon 5}$
Svensson & Häggkvist (1990)	1.0	—	1.95	—
Green (1992)	1.0	4.0	1.5	1.5
Kobayashi, Pereira & Siqueira (1994)[b]	1.0	—	0.975, <u>1.95</u>, 2.5	—
Liu et al. (1996)	1.0	4.0	1.5	1.5, <u>0.6</u>
Katul et al. (2004)[e]	1.0	4.0, 5.1	1.5, 0.9	1.5, 0.9
Foudhil, Brunet & Caltagirone (2005)	0.8	4.0	1.875	0.6, <u>0.81</u>, 1.5
Costa et al. (2006)[b]	1.0	—	1.95	—
Liang et al. (2006)	1.0	4.0	3.6	1.2
Sogachev & Panferov (2006)	1.0	4.0	1.52	1.833
Mochida et al. (2008)[c]	1.0	—	1.0, 1.5, <u>1.8</u>, 2.0	—
Mochida et al. (2008)[d]	1.0	4.0	1.5, <u>1.8</u>	0.6, 1.0 –<u>1.5</u>–1.8
Dalpé & Masson (2008)[d]	1.0	5.03	0.78	0.78
Rosenfeld, Marom & Bitan (2010)[e]	1.0	4.0	1.5	1.5
King, Tinoco & Cowen (2012)	0.2	1.0	—	—
Silva Lopes, Palma & Viana Lopes (2013)	—	4.0	—	0.9
Krayenhoff et al. (2015)[f]	1.0	6.5	1.26	1.26
Present study	—	2.67	—	1.0

Two-equation (k–ω) model	β_p	β_d	$C_{\varepsilon 4}$	$C_{\varepsilon 5}$
López & García (2001)	1.0	—	1.33	—
Neary (2003)	1.0/0.05	—	1.33/0.16	—
Sogachev (2009)	1.0	1.0	0.52	0.833
Sogachev, Kelly & Leclerc (2012)	1.0	1.0	0	−0.48

Second-order model	β_p	β_d	Transport equations	
Wilson & Shaw (1977)	1, 0, 0	—	$\overline{uu}$, $\overline{vv}$, $\overline{ww}$	
Yamada (1982)	0–1	—	$\overline{u_i u_j}$, ℓ	
Wilson (1988)[g]	>0	—	$\overline{u_i u_j}$	
Meyers & Baldocchi (1991)	1	—	$k - \overline{uw}$	
Ayotte, Finnigan & Raupach (1999)	—	—	$\overline{u_i u_j}$, ε	
Ayotte et al. (1999)	1	—	−1	

TABLE 1. Models and model coefficients in RANS formulation. Optimal values are underlined.
[a]Based on Wilson et al. (1998).
[b]Based on Svensson & Häggkvist (1990).
[c]Based on Yamada (1982) and Svensson & Häggkvist (1990).
[d]Based on Green (1992) and Liu et al. (1996).
[e]Based on Sogachev & Panferov (2006).
[f]Based on Sanz (2003).
[g]The mathematical formulation by Wilson (1988) differs from the other models.

Schumann 1992). According to Kanda & Hino (1994),

$$\mathcal{F}_e^{LES} = C_d a(z) \left(\alpha |\boldsymbol{U}|^3 - 2|\boldsymbol{U}|e \right), \tag{1.4}$$

where α, the ratio for the transformation of the energy loss in grid-scale flow through leaf drag to wake production in the subgrid-scale flow, can vary between 0 and 1. This equation is analogous to (1.2) and the coefficients α and 2 are denoted by β_p^{LES} and β_d^{LES}. It should be

mentioned that this analogy between (1.2) and (1.4) is merely formal, since k encompasses the whole range of scales whereas e is the TKE of subgrid scales. Most LES-based studies have their origin in the work of Shaw & Schumann (1992) and have used a simpler form of (1.4), in which β_p^{LES} is equal to 0 and β_d^{LES} is equal to 8/3 (e.g. Shaw & Patton 2003; Bohrer *et al.* 2009; Chatziefstratiou, Velissariou & Bohrer 2014; Nebenführ & Davidson 2015) or 2 (e.g. Shaw & Schumann 1992; Kanda & Hino 1994; Dwyer, Patton & Shaw 1997; Shen & Leclerc 1997; Patton *et al.* 1998; Yang *et al.* 2006; Dupont & Brunet 2008, 2009; Schrottle & Dornbrack 2013; Kanani *et al.* 2014; Schlegel *et al.* 2015; Boudreault *et al.* 2017). Unlike RANS-based studies (see table 1), very few LES-based studies take wake production into account (Shaw & Patton 2003). Concerning the constants (β_p^{LES} and β_d^{LES}) and their values, the uncertainty involved in LES-based modelling is much lower, since only one constant and two values (8/3 or 2) are used, and in the case of the subgrid-scale dynamic model (e.g. Yue *et al.* 2008; Silva Lopes *et al.* 2013, 2015; Yan *et al.* 2017) it does not even apply, because there is no equation for TKE of the subgrid scales (e). Concerning the uncertainty, even arbitrariness, as regards the constants in LES-based modelling, it is much lower, since only one constant (β_d^{LES}) and two values (8/3 or 2) are used, or, as is the case of the subgrid-scale dynamic model (e.g. Yue *et al.* 2008; Silva Lopes *et al.* 2013, 2015; Yan *et al.* 2017), this does not even apply, because there is no equation for TKE of the sub-grid scales (e).

Our goal in this work was to derive the most accurate equations for the effect a canopy has on a turbulent flow. The canopy-related terms in the equations, namely momentum, TKE and its dissipation rate, were approximated using a Taylor series expansion of the velocity magnitude, with a velocity scale based on the total kinetic energy. Unlike previous models (table 1), this approximation did not require any empirical coefficient. As in previous studies (Silva Lopes *et al.* 2013, 2015; Silva Lopes, Palma & Viana Lopes 2016), we considered LES to be a surrogate for a well-controlled experiment and we used the time-averaged LES results to validate the decomposition and determine the highest order required for an accurate representation of the effect of the trees in each of the three equations.

There are some similarities between ours and previous studies. For instance, Belcher, Jerram & Hunt (2003) and Belcher, Finnigan & Harman (2008) also made use of some form of decomposition in their linear versions of flow over forested regions. Our work is more similar to that of Lien *et al.* (2005), which addressed urban canopy flows. Both our study and that of Lien *et al.* (2005) decompose the canopy-related terms in a Taylor series and assume that the turbulent fluctuations are much smaller than the magnitude of the mean-flow velocity (weak turbulence regime). However, in this study, the velocity scale is different and validation, with a larger number of more demanding test cases, shows that the new approach does not suffer from the limitations raised by Lien *et al.* (2005) and that it can deal with low-velocity regions and flow-developing regions.

1.1. *Paper outline*

Section 2 addresses the canopy-related terms in the transport equations for momentum, Reynolds stresses, TKE and its dissipation rate, which are approximated by a Taylor series expansion in § 3. The quality of the expansion and the lowest order required for an accurate evaluation of the canopy effects are analysed in § 4, on the basis of LES results for the flow over a horizontally homogeneous forest, a forest edge and a forested hill. Section 5 presents a summary of our conclusions.

2. Mathematical model

A neutrally stratified flow within a forest is governed by equations expressing the conservation of mass and momentum:

$$\frac{\partial \langle u_i \rangle}{\partial x_i} = 0, \tag{2.1}$$

$$\frac{\partial \langle u_i \rangle}{\partial t} + \frac{\partial (\langle u_j \rangle \langle u_i \rangle)}{\partial x_j} = -\frac{1}{\rho}\frac{\partial \langle p \rangle}{\partial x_i} + \nu \frac{\partial^2 \langle u_i \rangle}{\partial x_j \partial x_j} - \frac{\partial \tau_{ij}}{\partial x_j} + f_i, \tag{2.2}$$

where u_i is the component of the velocity in the Cartesian direction x_i, p is the pressure, ρ and ν are the standard air density and kinematic viscosity and $\langle \; \rangle$ denotes a spatial filtering operation. Parameters $\tau_{ij} = \langle u_i u_j \rangle - \langle u_i \rangle \langle u_j \rangle$ are the LES subgrid stresses. The canopy drag force per unit mass f_i arises because filtering and derivation do not commute in the space occupied by the canopy elements. It is usually determined by

$$f_i = -C_d\, a(z)|\langle \boldsymbol{u} \rangle|\langle u_i \rangle, \tag{2.3}$$

where C_d is a drag coefficient (assumed constant, since form drag is much larger than viscous drag) and $|\langle \boldsymbol{u} \rangle| = (\langle u_i \rangle \langle u_i \rangle)^{1/2}$ is the scalar velocity. The spatial filtering over foliage elements used to obtain (2.1) and (2.2) was formalized by Wilson & Shaw (1977) and Raupach & Shaw (1982), and reviewed in detail by Finnigan & Shaw (2008).

After time averaging – denoted by an overbar – of the momentum equation (2.2),

$$\frac{\partial \overline{\langle u_i \rangle}}{\partial t} + \frac{\partial (\overline{\langle u_j \rangle \langle u_i \rangle})}{\partial x_j} = \frac{\mathrm{D}\overline{\langle u_i \rangle}}{\mathrm{D}t} = \cdots + \mathcal{F}_{u_i}, \tag{2.4}$$

the average canopy drag is found to be

$$\mathcal{F}_{u_i} = \overline{f_i} = -C_d a(z)\overline{|\langle \boldsymbol{u} \rangle|\langle u_i \rangle}. \tag{2.5}$$

Henceforth, we will drop the angle brackets that denote the filtering operation when referring to time averages of filtered quantities, i.e. $\bar{u}_i \equiv \overline{\langle u_i \rangle}$ and $\overline{u_i' u_j'} \equiv \overline{\langle u_i \rangle' \langle u_j \rangle'}$. The Reynolds stresses are $\overline{u_i' u_j'}$, where $u_i' = u_i - \bar{u}_i$ is the fluctuating part of the instantaneous velocity.

The counterpart of $\mathcal{F}_{u_i}$ in the transport equations for the Reynolds stresses $\overline{u_i' u_j'}$ is obtained in a similar manner to the other terms in these transport equations:

$$\overline{u_i'\frac{\mathrm{D}u_j'}{\mathrm{D}t}} + \overline{\frac{\mathrm{D}u_i'}{\mathrm{D}t}u_j'} = \frac{\mathrm{D}\overline{u_i' u_j'}}{\mathrm{D}t} = \cdots + \mathcal{F}_{u_i' u_j'}, \tag{2.6}$$

where

$$\mathcal{F}_{u_i' u_j'} = \overline{u_i' f_j + u_j' f_i} \tag{2.7}$$

is the correlation between canopy drag and velocity fluctuations. In the same way, for each component ε_{ij} of the Reynolds stresses dissipation rate tensor,

$$\overline{2\nu\frac{\partial u_i'}{\partial x_k}\frac{\mathrm{D}}{\mathrm{D}t}\left[\frac{\partial u_j'}{\partial x_k}\right]} + \overline{\frac{\mathrm{D}}{\mathrm{D}t}\left[\frac{\partial u_i'}{\partial x_k}\right]\frac{\partial u_j'}{\partial x_k}} = \frac{\mathrm{D}}{\mathrm{D}t}\overline{2\nu\frac{\partial u_i'}{\partial x_k}\frac{\partial u_j'}{\partial x_k}} = \frac{\mathrm{D}\varepsilon_{ij}}{\mathrm{D}t} = \cdots + \mathcal{F}_{\varepsilon_{ij}}, \tag{2.8}$$

with

$$\mathcal{F}_{\varepsilon_{ij}} = 2\nu\overline{\frac{\partial u_i'}{\partial x_k}\frac{\partial f_j}{\partial x_k} + \frac{\partial u_j'}{\partial x_k}\frac{\partial f_i}{\partial x_k}} \tag{2.9}$$

being responsible for the enhancement of dissipation by the correlation between the gradient of the canopy drag and the turbulent strain rate. Finally, the terms that correspond to the action of the canopy drag on the TKE (or k) and on its dissipation rate (ε) are obtained by contracting (2.7) and (2.9) for $\langle u_i' u_i' \rangle$ and ε_{ii}:

$$\mathcal{F}_k = \overline{u_i' f_i} = -C_d\, a(z) \overline{|\boldsymbol{u}| u_i u_i'}, \tag{2.10}$$

$$\mathcal{F}_\varepsilon = 2\nu \overline{\frac{\partial u_i'}{\partial x_k} \frac{\partial f_i}{\partial x_k}} = -2\nu C_d \overline{\frac{\partial}{\partial x_k} [a(z)|\boldsymbol{u}| u_i] \frac{\partial u_i'}{\partial x_k}}. \tag{2.11}$$

Because f_i (equation (2.3)) results from the spatial filtering, $\mathcal{F}_k$ and $\mathcal{F}_\varepsilon$ only represent the canopy action at larger scales. This means that $\mathcal{F}_k$ cannot account for the increased turbulent production caused by enhanced strain of the flow in the space between leaves – wake production. However, such small-scale turbulence should dissipate quickly (over a short distance) and contribute little to TKE transport (Raupach & Shaw 1982; Wilson 1988; Shaw & Patton 2003).

3. Weak turbulence regime

Since the canopy-related terms (equations (2.3), (2.10) and (2.11)) depend on the velocity magnitude, Lien & Yee (2005) introduced an approximation for $|\boldsymbol{u}|$ based on perturbation theory:

$$|\boldsymbol{u}| = U\sqrt{1 + 2\frac{u_s'}{U} + \frac{u_i' u_i'}{U^2}}, \tag{3.1}$$

where $U = (U_i U_i)^{1/2}$ is the magnitude of the mean velocity ($U_i = \bar{u}_i$) and u_s' and u_n', given by

$$u_s' \equiv u_i' \frac{U_i}{U} \quad \text{and} \quad u_n' \equiv \left(u_i' u_i' - u_s' u_s'\right)^{1/2}, \tag{3.2a,b}$$

are the velocity fluctuations along the streamwise and normal directions defined by the mean flow. Using a series expansion of the square root in (3.1), Lien & Yee (2005) expressed the canopy-related terms in the transport equations of a RANS model as the sum of time-averaged second-order velocity moments. The expansion about the mean flow state assumes that the turbulent fluctuations are much smaller than the magnitude of the mean-flow velocity – weak turbulence regime (WTR):

$$u_i' u_i' \ll U^2. \tag{3.3}$$

This approach can be applied near the surface, because both the mean velocity and the fluctuations approach zero. However, in a region of separated flow, as on the lee side of a hill covered with vegetation, the turbulent fluctuations can be large and the mean velocity small, or even null, which breaks the WTR assumption (3.3).

Here, we propose to redefine the velocity scale (3.1), expanding $|\boldsymbol{u}|$ around a velocity Q, derived from the total kinetic energy (mean flow + turbulence):

$$|\boldsymbol{u}| = Q\sqrt{1 + 2\frac{U u_s'}{Q^2} + \frac{u_i' u_i' - 2k}{Q^2}}, \tag{3.4}$$

with $Q = (U^2 + 2k)^{1/2}$. We define ξ and η such that

$$\xi = \frac{Uu'_s}{Q^2} \quad \text{and} \quad \eta = \frac{u'_i u'_i - 2k}{Q^2}, \tag{3.5a,b}$$

which will be used as the small parameters required to perform the Taylor series expansion of the square root:

$$\sqrt{1 + 2\xi + \eta} \approx 1 + \xi + \frac{\eta - \xi^2}{2} + \frac{\xi^3 - \xi\eta}{2} + \frac{6\xi^2\eta - \eta^2 - 5\xi^4}{8} + \cdots. \tag{3.6}$$

In the case of Lien & Yee (2005) (3.1), the expansion of the fluctuating term has a non-zero average, yielding an expansion around zero, fluctuations and a poor quality of series convergence. In (3.4), we reorganized the argument of the square root to have a fluctuating term around zero and a greater velocity scale ($Q > U$). Expanding with the rescaled fluctuating term leads to a better convergence of the Taylor series.

An indication of the validity of the approximation can be inferred from the joint probability distribution of velocity fluctuations in a LES of a horizontally homogeneous canopy. In a statistically steady-state regime, the velocity fluctuations are well described by a probability distribution that is a function only of the distance to the ground z. The probability distribution is given by

$$P(\boldsymbol{u}|\boldsymbol{r}) = \lim_{T \to \infty} \frac{1}{T} \int_t^{t+T} \delta(\boldsymbol{u}'(\boldsymbol{r}, t') - \boldsymbol{u}) \, \mathrm{d}t' \tag{3.7}$$

and any average of the fluctuations at a point in space, $\boldsymbol{r}$, can be obtained by a phase-space average:

$$\bar{A}(\boldsymbol{r}) = \int A(\boldsymbol{u}')P(\boldsymbol{u}'|\boldsymbol{r}) \, \mathrm{d}\boldsymbol{u}', \tag{3.8}$$

where A is a generic function of the velocity.

A Taylor series expansion of the operator $A(\boldsymbol{u}')$ is valid if the higher orders of the series expansion are a good approximation in the regions where the probability weight is relevant. Figure 1 shows the joint probability distribution of the streamwise and normal components of the velocity fluctuations (obtained from LES results, as in § 4.2) at the location where the turbulence is strongest. We can observe that the probability weight is concentrated near the origin, where the instantaneous velocity is equal to the mean velocity. This measure suggests the approximation based on small velocity fluctuations (WTR) is valid and shows that the distribution is concentrated in a region inside the average fluctuation (u'_s, u'_n) and that the reduced variables ξ and η (equation (3.5)) will be small even when the mean velocity U is small.

3.1. *Transport of momentum*

Although (2.3) has been used to model the canopy drag with both the LES (Shaw & Schumann 1992; Kanda & Hino 1994; Dwyer *et al.* 1997; Patton *et al.* 1998) and RANS (Wilson 1988; Svensson & Häggkvist 1990; Green 1992) methods, it does not yield the same time-averaged force since $|\bar{\boldsymbol{u}}|\bar{u}_i \leq \overline{|\boldsymbol{u}|u_i}$, as signalled by Su *et al.* (1998) and Finnigan & Shaw (2008), who suggested using a lower C_d with LES.
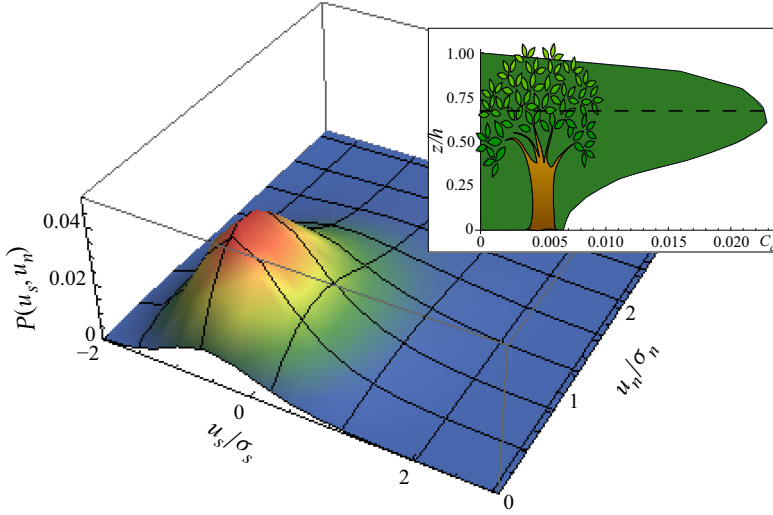
FIGURE 1. Joint probability density function of the streamwise and normal velocity components (u'_s, u'_n) of the flow inside a horizontally homogeneous forest.

Here, we use the WTR assumption and the expansion (3.6) to propose an alternative formulation for (1.1) in the RANS framework, in order to match the LES results. The canopy drag (2.5) can be expressed as a sum of terms with a decreasing order of magnitude:

$$\mathcal{F}_{U_i} = \lim_{n \to +\infty} S_{U_i}(n), \tag{3.9}$$

where the n-truncated Taylor expansion,

$$S_{U_i}(n) = -C_d\, a(z) \sum_{j=0}^{n} s_{U_i}(j), \tag{3.10}$$

is generated by the expansion of the square root (3.6):

$$\frac{\overline{|u|u}}{Q} = U_i\overline{\sqrt{1 + 2\xi + \eta}} + \overline{u_i\sqrt{1 + 2\xi + \eta}}. \tag{3.11}$$

Collecting order by order, the first four terms of (3.10) are

$$s_{U_i}(0) = QU_i, \tag{3.12a}$$

$$s_{U_i}(1) = 0, \tag{3.12b}$$

$$s_{U_i}(2) = \frac{U}{Q}\left(\overline{u'_s u'_i} - \frac{U U_i}{2Q^2}\overline{u'_s u'_s}\right) = \frac{U_j}{Q}\left(\delta_{ik} - \frac{U_i U_k}{2Q^2}\right)\overline{u'_j u'_k}, \tag{3.12c}$$

$$s_{U_i}(3) = \frac{1}{2Q}\left(\overline{u'_i u'_j u'_j} - \frac{U^2}{Q^2}\overline{u'_s u'_s u'_i}\right)$$

$$= \frac{1}{2Q}\left(\delta_{ij} - \frac{U_i U_j}{Q^2}\right)\left(\delta_{kl} - \frac{U_k U_l}{Q^2}\right)\overline{u'_j u'_k u'_l}. \tag{3.12d}$$

The zeroth-order term (3.12a) agrees with the common RANS canopy drag (1.1) when the TKE is much lower than the kinetic energy of the mean field ($k \ll U^2$, $Q \approx U$). However, there is numerical (see figure 1 of Silva Lopes *et al.* (2013)) and experimental (see figure 3 of Cescatti & Marcolla (2004)) evidence that the ratio between turbulent (k) and mean field kinetic ($1/2U^2$) energies could reach between 10 and 100 %. The differences emerge when higher-order terms are considered: for instance, the second-order term (3.12c) of the WTR expansion predicts an average finite drag normal to the flow direction if the two velocity components are correlated, i.e. the Reynolds shear stress $\overline{u'_s u'_n}$ is not null. This cannot be predicted by (1.1), the basis of the RANS canopy models. Although the normal component is one order of magnitude smaller than the streamwise component (as shown by the LES results in § 4.2), this is a major conceptual difference between this formulation and the common RANS approach (1.1).

3.2. *Transport of TKE*

Following the same procedure as in § 3.1, a series expansion can also be obtained for the rate of work done by the canopy drag against the turbulent fluctuations (2.10):

$$S_k(n) = -C_d \, a(z) \sum_{j=0}^{n} s_k(j), \tag{3.13}$$

where

$$s_k(0) = 2Qk, \tag{3.14a}$$

$$s_k(1) = 0, \tag{3.14b}$$

$$s_k(2) = \frac{U^2(Q^2 - k)}{Q^3}\overline{u'^2_s}, \tag{3.14c}$$

$$s_k(3) = \frac{U(3Q^2 - 2k)}{2Q^3}\overline{u'_s u'_i u'_i} - \frac{U^5}{2Q^5}\overline{u'^3_s}, \tag{3.14d}$$

$$s_k(4) = \frac{U^4(2Q^2 - 5k)}{4Q^7}\overline{u'^4_s} - \frac{U^2(2Q^2 - 3k)}{2Q^5}\overline{u'^2_s(u'_i u'_i - 2k)} + \frac{2Q^2 - k}{4Q^3}\left[\overline{(u'_i u'_i)^2} - 4k^2\right]. \tag{3.14e}$$

If the TKE is much lower than the kinetic energy of the mean field ($k \ll U^2$, $Q \approx U$) and isotropy is assumed, the second-order approximation is identical to the RANS k–ε canopy models (1.2) without wake production ($\beta_p = 0$). This is a consequence of the assumptions of our mathematical model (§ 2) and agrees with the LES results obtained by Silva Lopes *et al.* (2013), in whose work the canopy was also modelled as a homogeneous porous medium. Wake production is due to horizontal heterogeneity of the vegetation and exists at scales much smaller than the grid sizes currently used in the simulation of atmospheric flows. This is different from canopy-resolving LES as applied to rod or urban canopy flows (e.g. Novak *et al.* 2000; Castro, Cheng & Reynolds 2006; Cava & Katul 2008; Bou-Zeid *et al.* 2009; Patton *et al.* 2011; Poggi, Katul & Vidakovic 2011; Blackman *et al.* 2017). Truncating the series to second order requires only quantities that can be obtained from RANS models. Third-order terms can also be included if an approximation for the third-order correlations is used.

3.3. *Transport of the dissipation rate of TKE*

Finally, an approximation for the effect of the canopy drag on the transport of TKE dissipation rate (2.11) was also derived:

$$S_\varepsilon(n) = -\nu \, C_d \sum_{j=0}^{n} s_\varepsilon(j). \tag{3.15}$$

The expansion of the product between the gradient of the canopy drag and the turbulent strain rate is more complex than that for momentum or TKE transport. For the sake of convenience (§ 4.4), the series terms were split into large-scale contribution, $S_\varepsilon^L(n)$, which depends on velocity correlations, and small-scale contribution, $S_\varepsilon^s(n)$, which depends on statistics that include the turbulent strain rate:

$$S_\varepsilon(n) = S_\varepsilon^L(n) + S_\varepsilon^s(n) = -\nu \, C_d \left(\sum_{j=0}^{n} s_\varepsilon^L(j) + \sum_{j=0}^{n} s_\varepsilon^s(j) \right), \tag{3.16}$$

where

$$s_\varepsilon^L(0) = s_\varepsilon^L(1) = 0, \tag{3.17a}$$

$$s_\varepsilon^L(2) = \frac{\partial}{\partial x_k} \left[a(z) Q \left(\frac{U_i U_j}{Q^2} + \delta_{ij} \right) \right] \frac{\partial \overline{u_i' u_j'}}{\partial x_k}, \tag{3.17b}$$

$$s_\varepsilon^L(3) = \frac{\partial}{\partial x_l} \left[a(z) \frac{U_i}{Q} \left(\delta_{jk} - \frac{U_j U_k}{3Q^2} \right) \right] \frac{\partial \overline{u_i' u_j' u_k'}}{\partial x_l} \tag{3.17c}$$

and

$$s_\varepsilon^s(0) = s_\varepsilon^s(1) = 0, \tag{3.18a}$$

$$s_\varepsilon^s(2) = 2a(z) Q \left(\delta_{ij} + \frac{U_i U_j}{Q^2} \right) \overline{\frac{\partial u_i'}{\partial x_k} \frac{\partial u_j'}{\partial x_k}}, \tag{3.18b}$$

$$s_\varepsilon^s(3) = 2a(z) \left(\frac{U_i \delta_{jk} + U_j \delta_{ik} + U_k \delta_{ij}}{Q} - \frac{U_i U_j U_k}{Q^3} \right) \overline{u_i' \frac{\partial u_j'}{\partial x_l} \frac{\partial u_k'}{\partial x_l}}. \tag{3.18c}$$

As with TKE transport, if the TKE is much lower than the kinetic energy of the mean field ($k \ll U^2$, $Q \approx U$) and isotropy of both the Reynolds stresses and TKE dissipation rate is assumed, the second-order small-scale approximation becomes similar to conventional RANS k–ε canopy models without wake production (equation (1.3)). As will be shown in § 4.4, the magnitude of the small-scale part overshadows the large-scale part, since dissipation is mainly effected at the smaller scales. Also, if isotropy is assumed, the second-order approximation uses quantities available in RANS models. The correlations required by the third-order small-scale term are difficult to approximate.

4. Numerical experiments and validation

Large-eddy simulations were performed (table 2) to assess the accuracy of the proposed model (equations (3.12), (3.14), (3.17) and (3.18)), that is, the function of the order of

	Horizontally homogeneous	Forest edge	Forested hill
Domain size	$9.6h \times 4.8h \times 3h$	$38.4h \times 19.2h \times 6.2h$	$300h \times 60h \times 20h$
h (m)	20	7.5	10.0
U_b (m s^{-1})	2	3	2
C_d	0.15	0.2	0.2
LAI	2	2	1.6
Grid nodes	$192 \times 96 \times 98$	$960 \times 480 \times 204$	$1698 \times 252 \times 340$
z_0/h	1.00×10^{-3}	3.73×10^{-3}	3.0×10^{-3}
$\Delta x/h = \Delta y/h$	5.00×10^{-2}	4.00×10^{-2}	1.77×10^{-1}
$\Delta z_{min}/h$	1.25×10^{-2}	5.33×10^{-3}	1.77×10^{-2}
$f_{z_{max}}$	1.045	1.031	1.017

TABLE 2. Numerical parameters. Here U_b, bulk velocity; $LAI = \int_0^h a(z)\, \mathrm{d}z$, leaf area index; $f_{z_{max}}$, maximum expansion factor of the grid in the vertical direction.

approximation in the description of canopy effects on the transport of momentum, TKE and its dissipation rate. Three different flows – over a horizontally homogeneous canopy, a forest edge and a forested hill – were considered on the basis of studies by Shaw & Schumann (1992), Yang *et al.* (2006) and Dupont, Brunet & Finnigan (2008), respectively. These flows have already been considered by Silva Lopes *et al.* (2013), because they test the accuracy of the model for flows from the simplest to one with pressure gradients, streamline curvature and separation. The results obtained by Silva Lopes *et al.* (2013) and their set of optimized coefficients, identified as reference RANS k–ε, will serve as an additional source for comparing the performance of the decomposition.

4.1. *Numerical model*

The numerical model is composed of (2.1) and (2.2) and the subgrid stresses, modelled by an eddy-viscosity assumption:

$$\tau_{ij} - \tfrac{1}{3}\delta_{ij}\tau_{kk} = -2\nu_t S_{ij} = -2\left(C\Delta\right)^2 |S|S_{ij}, \tag{4.1}$$

where $\Delta = (\Delta x\, \Delta y\, \Delta z)^{1/3}$ is the filter size, $S_{ij} = (\partial u_i/\partial x_j + \partial u_j/\partial x_i)/2$ is the resolved strain-rate tensor and $|S| = (2S_{ij}S_{ij})^{1/2}$ is its magnitude. The coefficient C was obtained using a combination of the Meneveau, Lund & Cabot (1996) Lagrangian dynamic model with the wall-damped Mason & Thomson (1992) Smagorinsky model near the surface. The two models merged below $0.75h$ and $C_S = 0.16$ was used in the Smagorinsky model. Further details of the implementation can be found in Silva Lopes, Palma & Castro (2007) and Silva Lopes *et al.* (2013). Periodic conditions were used in the streamwise and spanwise directions. The surface stress was determined using the Marusic, Kunkel & Porté-Agel (2001) model, while the top of the domain used a free-slip condition. At each time step, a uniform (in space) streamwise pressure gradient was determined to balance the canopy drag, resulting in a constant flow rate (momentum balance).

Numerical uncertainty has been assessed previously (Silva Lopes *et al.* 2013), on the basis of the streamwise velocity normalized with the volume-averaged streamwise velocity component (U_b), and the TKE and Reynolds shear stress ($u'_s u'_n$). Both of these were normalized with the friction velocity (u_*), calculated using the total shear stress (resolved and subgrid) at the canopy top. Calculations in three numerical grids of increasing
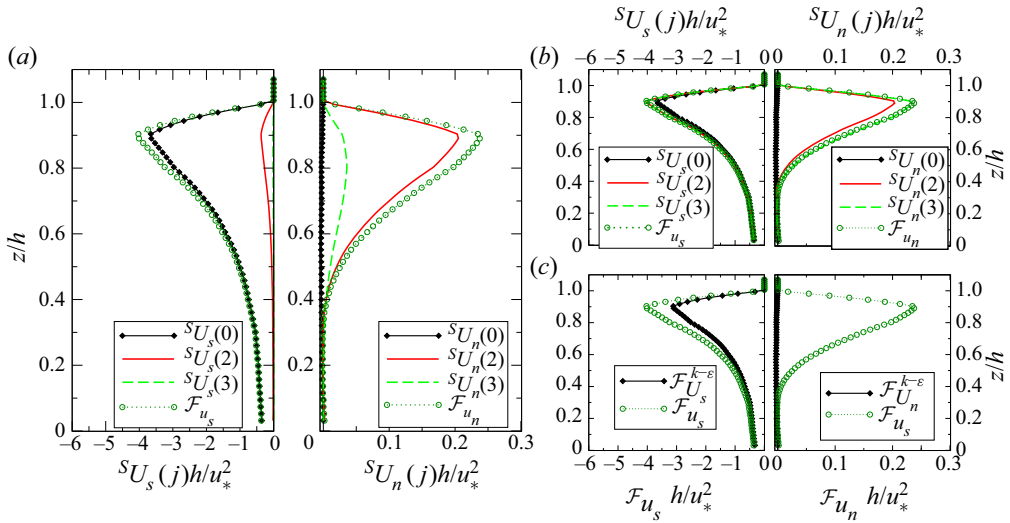
FIGURE 2. Approximations of the canopy drag along the streamwise and normal directions (*s* and *n*) in the horizontally homogeneous forest. (*a*) The WTR series terms up to the third order (s_{U_i} (3.12)) and LES results ($\mathcal{F}_{U_i}$ (2.5)); (*b*) WTR summations up to the third order (S_{U_i} (3.10)) and LES results; (*c*) reference RANS *k–ε* ($\mathcal{F}_{U_i}^{k-\varepsilon}$ (1.1)) and LES results ($\mathcal{F}_{U_i}$ (2.5)). Note that horizontal scales are magnified 20× in the case of quantities referring to the normal direction, *n*.

resolution, of which the finest was identical to the one in this study, showed that U/U_b and $u_s' u_n'/u_*^2$ were independent of grid resolution. In contrast, k/u_*^2 above the canopy increased nearly 10 % in peak value between the coarsest grid ($96 \times 48 \times 48$) and finest grid ($192 \times 96 \times 98$) results. The contribution of the subgrid stress to the peak Reynolds shear stress, at treetop level, decreased from 4 % with the coarsest grid to 2 % with the finest. The grid refinement study was performed for the horizontally homogeneous canopy, while in the other cases, the resolution was limited by computational resource availability. It was, nevertheless, considered appropriate for this study.

4.2. *Transport of momentum*

Figure 2 shows the WTR approximation of the canopy drag along the streamwise and normal directions in the horizontally homogeneous forest, where there is no streamline curvature, and a comparison with LES results. Regardless of the direction, the magnitude of the series terms decreases with the order and the sum approaches the LES results (figure 2*a,b*), suggesting the convergence of the series. The WTR expansions correctly predicted both drag components, with the largest terms being based on the streamwise velocity and on the Reynolds shear stress $\overline{u'w'}$. The zeroth order was sufficient to improve the standard RANS approximation, which underpredicted streamwise drag by 25 % (figure 2*c*).

In the case of the forest edge and the forested hill, with streamline curvature, it is useful to analyse the drag force in terms of its streamwise and normal components:

$$\mathcal{F}_{U_s}(n) = S_{U_i}(n)\frac{U_i}{U} \quad \text{and} \quad \mathcal{F}_{U_n}(n) = \left[|\mathbf{S}_U(n)|^2 - \mathcal{F}_{U_s}^2(n)\right]^{1/2}, \qquad (4.2a,b)$$
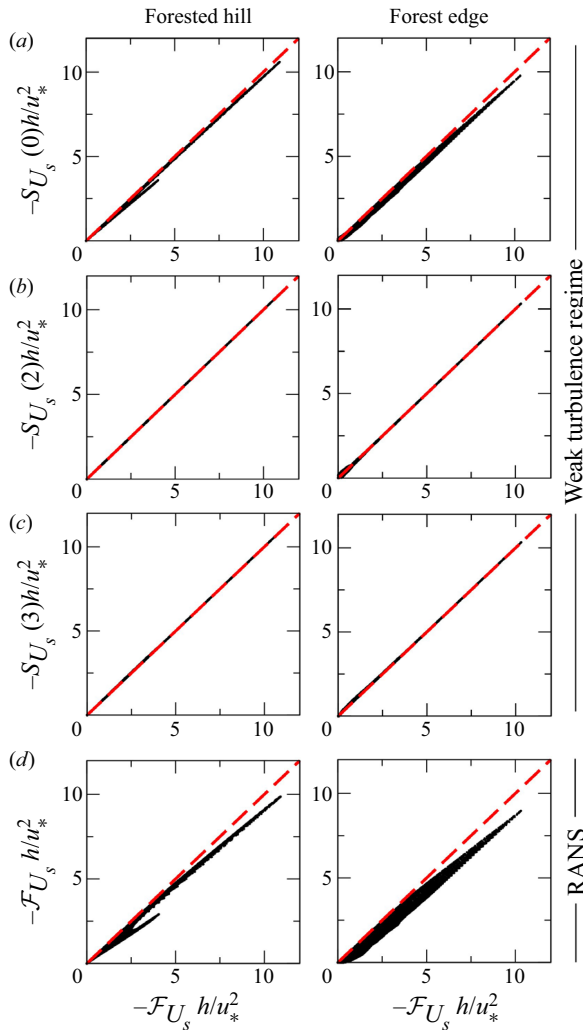
FIGURE 3. Correlations of approximations of the streamwise component of the canopy drag in the forest edge and forested hill flows. (*a–c*) The WTR summations up to the third order (S_{U_s} (3.10)) and LES results ($\mathcal{F}_{U_s}$ (2.5)); (*d*) reference RANS k–ϵ ($\mathcal{F}_{U_s}^{k-\epsilon}$ (1.1)) and LES results.

and to study canopy force modelling by verifying the correlation of the WTR expansion up to the third order (3.10) with the canopy drag determined in the LES simulations at each point within the canopy layer (figures 3 and 4). In the case of the streamwise component, a perfect match is already achieved by the second-order WTR approach (figure 3*b*,*c*), whereas the standard RANS presented deviations of up to 20 % (figure 3*d*). The normal component was around $20\times$ smaller than the streamwise one (as in the horizontally homogeneous canopy flow) and the convergence was slower, especially in the case of the forested hill (figure 4). However, the dispersion observed in the correlation was, in either case, restricted to specific regions of the physical domain (the leading edge of the forest and the lee side of the forested hill, inside the separated flow region).

In summary and on the basis of the three flow cases, we conclude that accurate modelling of the canopy drag based on the WTR expansion required a second-order
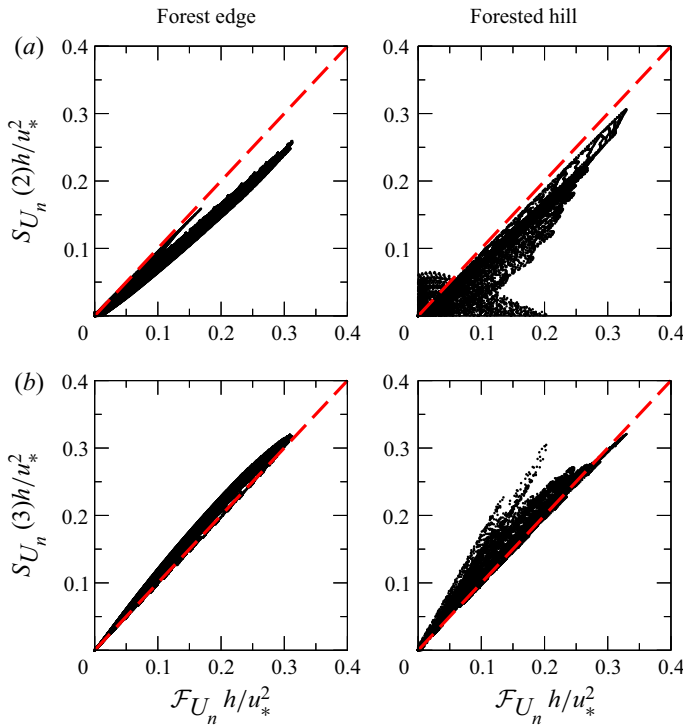
FIGURE 4. Correlations of approximations of the normal component of canopy drag in the forest edge and forested hill flows. (*a*) Second-order and (*b*) third-order WTR summations (S_{U_n} (3.10)) and LES results ($\mathcal{F}_{U_n}$ (2.5)).

approximation of the streamwise component and a fourth-order approximation of the normal component. This may be compared with the standard RANS approach, which was less accurate than the zeroth-order WTR for the streamwise component and does not predict any drag in the normal direction.

4.3. *Transport of TKE*

As with canopy drag, there is evidence of convergence of the WTR approximation of the effect on TKE transport in the horizontally homogeneous canopy flow, since the magnitude of the terms decreased with order and their sum approached the LES results (figure 5*a*,*b*). However, convergence was slower than for canopy drag (figure 2) and the third order was required to capture 95.8 % of the LES results, compared to 83.5 % in the case of the second order (figure 5*b*). Also, the WTR approximation could not improve on the reference RANS model prediction of Silva Lopes *et al.* (2013):

$$\mathcal{F}_k^{k-\varepsilon} = -C_d \, a(z) \, \beta_d |U| k, \tag{4.3}$$

in which the constant $\beta_d = 4.0$ was calibrated with this flow (figure 5*c*).

In the more complex cases, the flows over the forest edge and the forested hill, the findings of the horizontally homogeneous canopy flow were confirmed, with the third order providing a good approximation and the fourth order matching the LES results (figure 6*c*,*d*). In these cases, the WTR approximation improved the reference RANS model
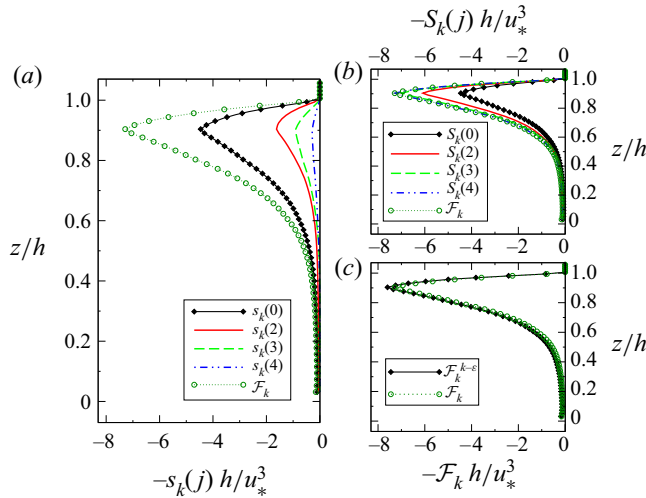
FIGURE 5. Approximations of the contribution of canopy drag to TKE transport in the horizontally homogeneous forest. (*a*) The WTR series terms up to the fourth order (s_k (3.14)) and LES results ($\mathcal{F}_k$ (2.10)); (*b*) WTR summations up to the fourth order (S_k (3.13)) and LES results; (*c*) reference RANS k–ε ($\mathcal{F}_k^{k-\varepsilon}$ (4.3)) and LES results.

predictions (figure 6*e*), which failed mainly at the edge of the forest and in the separation on the lee side of the hill. However, we note that the third-order term requires velocity correlations of the same order.

4.4. *Transport of dissipation rate of TKE*

The WTR approximation of the effect of canopy drag on the transport of the dissipation rate of TKE includes only second- and higher-order terms (equations (3.17) and (3.18)). As in the transport of momentum or TKE, the magnitude of the third-order term was smaller than the second-order term and their sum approached the LES result in the horizontally homogeneous canopy flow (figure 7*a*,*b*), indicating convergence of the series. The second-order term of the series, (3.17*b*) and (3.18*b*), the first non-zero terms of the series, yielded a result within 83.8 % of the peak value (figure 7*b*). The LES results were mimicked by either the WTR third-order approximation (99.6 %) or the reference RANS model prediction of Silva Lopes *et al.* (2013):

$$\mathcal{F}_\varepsilon^{k-\varepsilon} = -C_d a(z) C_{\varepsilon 5} \beta_d |U| \varepsilon, \tag{4.4}$$

in which the constant $C_{\varepsilon 5} = 0.9$, such as β_d (4.3), was calibrated also with this flow (figure 7*c*).

For the forest edge and forested hill flows, the second-order WTR approximation was sufficient to improve the correlation of the reference RANS model, which showed considerable dispersion (figure 8). However, we note that the second-order WTR approximation requires knowledge of turbulent strain rate correlations and the third-order approximation requires third-order statistics including the turbulent strain rate and velocity fluctuations.
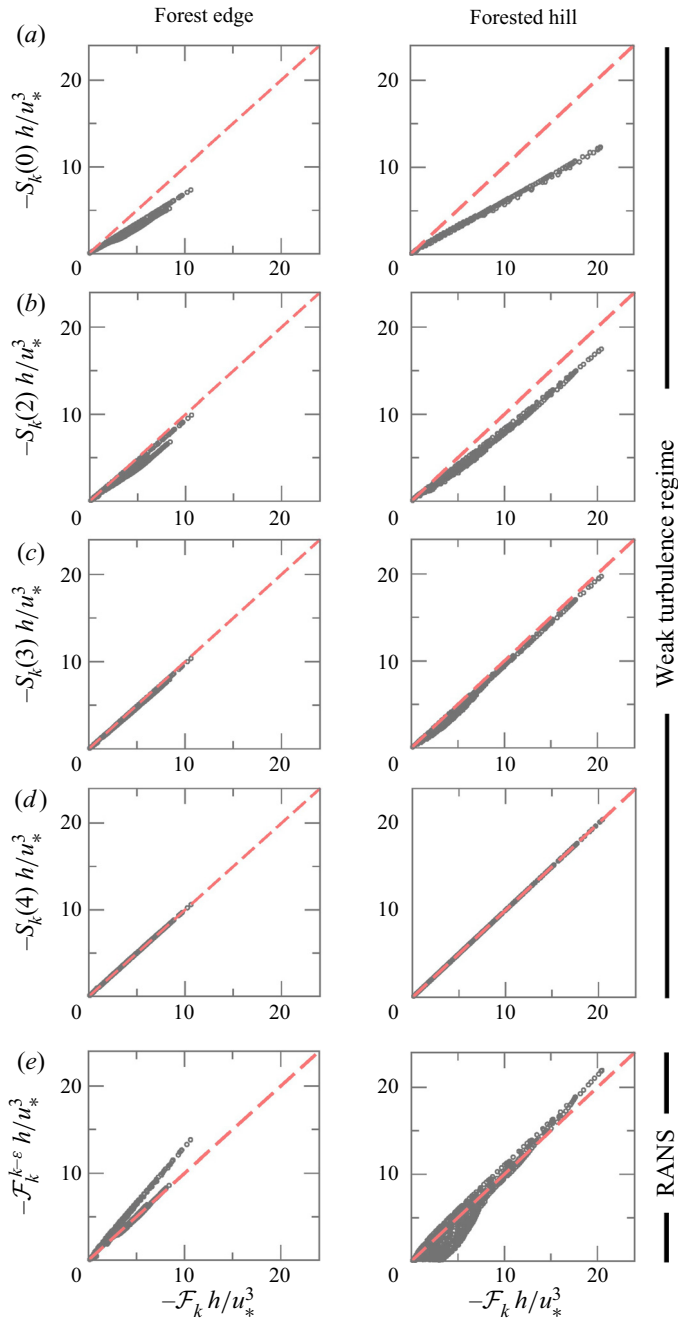
FIGURE 6. Correlations of approximations of the contribution of canopy drag to TKE transport in the forest edge and forested hill flows. (*a–d*) The WTR summations up to the fourth order (S_k (3.13)) and LES results ($\mathcal{F}_k$ (2.10)); (*e*) reference RANS k–ε ($\mathcal{F}_k^{k-\varepsilon}$ (4.3)) and LES results ($\mathcal{F}_k$ (2.10)).
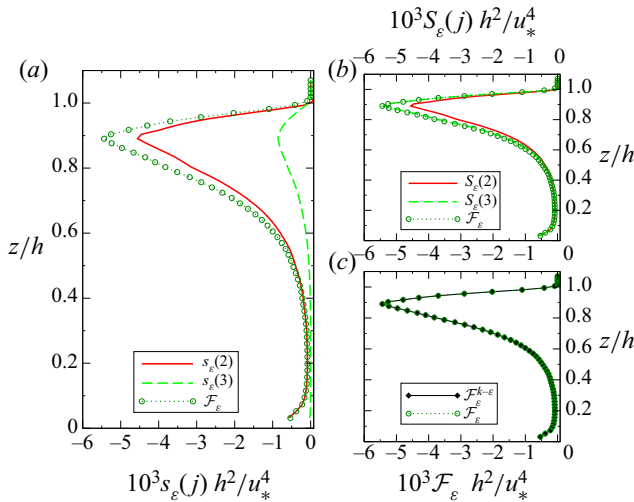
FIGURE 7. Approximations of the contribution of canopy drag to the transport of the TKE dissipation rate in the horizontally homogeneous forest. (*a*) The WTR series terms up to the third order (s_ε (3.17) and (3.18)) and LES results ($\mathcal{F}_\varepsilon$ (2.11)); (*b*) WTR summations up to the third order (S_ε (3.16)) and LES results ($\mathcal{F}_\varepsilon$ (2.9)); (*c*) reference RANS k–ε ($\mathcal{F}_\varepsilon^{k-\varepsilon} k$ (1.3)) and LES results ($\mathcal{F}_\varepsilon$ (2.9)).

Additionally, in assessing the accuracy of the WTR approximation to the effect of canopy drag on the transport of TKE dissipation rate, we must bear in mind that this involves mainly small scales, which can be shown by the dependence of the WTR approximation on the turbulent strain rate correlations (3.18*c*). This is the opposite of the effect on the transport of momentum and TKE, which depends on velocity correlations and concerns mainly large scales. As such, a grid refinement study was performed on the horizontally homogeneous canopy flow, to check whether the accuracy of the WTR approximation varied with resolved dissipation. Three different grid resolutions were considered: low resolution (LR; $136 \times 68 \times 70$), medium resolution (MR; $192 \times 96 \times 98$) and high resolution (HR; $272 \times 136 \times 138$ nodes); i.e. the grid space was nearly two times larger in the LR grid than in the HR grid. As expected, the small-scale part of the WTR approximation (s_ε^s) increased with the grid resolution (figure 9*a*), whereas the large-scale part (s_ε^L), already properly resolved on the LR grid, remained almost constant (figure 9*b*). Nevertheless, there was always a good agreement between the WTR approximation determined using resolved LES fields and the LES results on the same grid.

As regards the grid refinement study (figure 9), if a major part of the dissipation were to be resolved, we would expect that: (a) the agreement between the WTR approximation and LES results would persist and (b) the small-scale part of the WTR approximation would overshadow the large-scale part (cf. figure 9*a* with figure 9*b*). This latter consideration can be used in the construction of a RANS model, based solely on the small-scale part. We note, however, that if the grid resolution of the LES was increased to approach the dissipative scales of the flow, the field-scale approach, used to model the forest canopy, should be replaced by the plant-scale approach (Yue *et al.* 2007). In this approach, the local canopy structure is taken into account instead, rather than a horizontally homogeneous drag field.
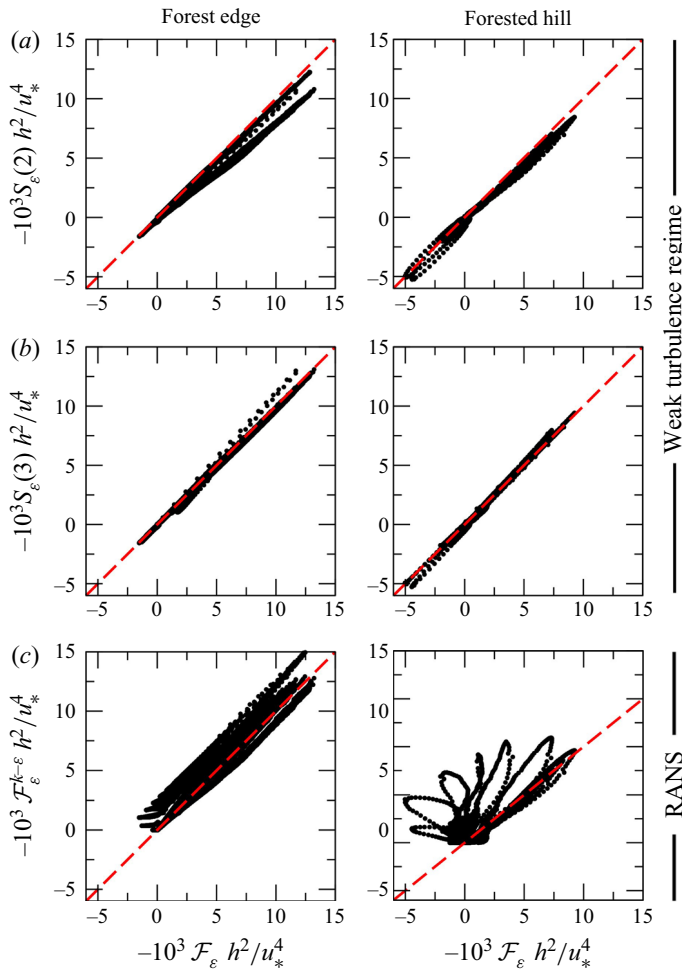
FIGURE 8. Correlations of approximations of the contribution of canopy drag to TKE dissipation rate transport in the forest edge and forested hill flows. (*a*) Second-order and (*b*) third-order WTR summations (S_ε (3.16)) and LES results ($\mathcal{F}_\varepsilon$ (2.11)); (*c*) reference RANS k–ε ($\mathcal{F}_\varepsilon^{k-\varepsilon}$ (1.3)).

In the cases of the forest edge and forested hill flows (figure 10), the large- and small-scale contributions, determined using the resolved LES fields, were of a similar magnitude and only their sum correlated well with LES results. This occurred because the spatial resolution was not as good as it was for the horizontally homogeneous canopy flow. This is why fewer small scales and, consequently, dissipation were resolved.

4.5. *Comparison with conventional RANS models*

The WTR approximations are similar to conventional RANS k–ε canopy models if certain assumptions are made: (a) the TKE is much smaller than the kinetic energy of the mean field: $k \ll U^2$, $Q \approx U$); (b) the Reynolds stress and its dissipation rate tensors are isotropic: $\overline{u_i'u_j'} = 2/3k\delta_{ij}$ and $\varepsilon_{ij} = 2/3\varepsilon\delta_{ij}$; and (c) the large-scale contribution to the effect on the transport of TKE dissipation rate is much smaller than the small-scale part (see above):
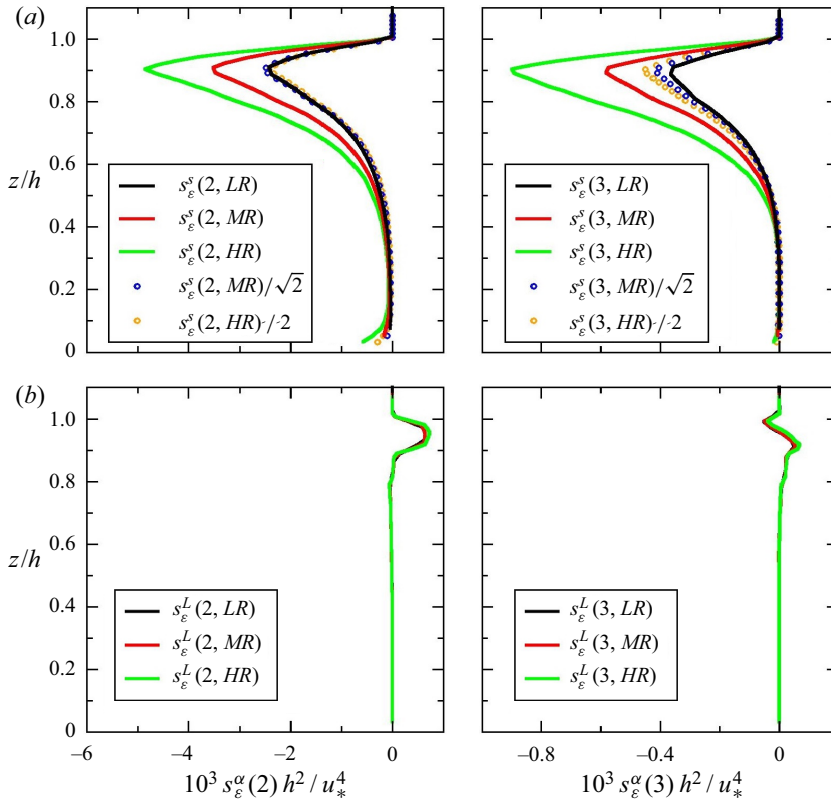
FIGURE 9. WTR approximations of the contribution of canopy drag to TKE dissipation rate transport in the horizontally homogeneous forest with different grid resolutions (LR, MR and HR). (*a*) Second- and third-order small-scale series terms (s_ε^s (3.18)); (*b*) Second- and third-order large-scale series terms (s_ε^L (3.17)). Note that the horizontal scale is magnified 6× in the case of the third-order terms.
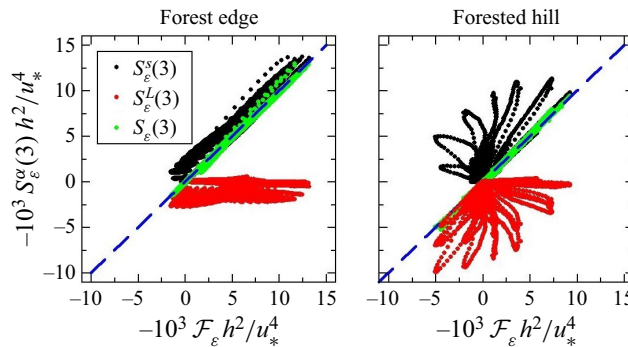

FIGURE 10. Forest edge and forested hill. Correlation between the contribution of canopy drag to TKE dissipation rate transport predicted by the WTR expansion up to the third order (S_ε(3) (3.15)) and LES results ($\mathcal{F}_\varepsilon$ (2.11)). Contribution of small-scale (S_ε^s(3) (3.16)) and large-scale (S_ε^L(3) (3.16)) components, and sum of both of these.

$S_\varepsilon^L \ll S_\varepsilon^s$, $S_\varepsilon \approx S_\varepsilon^s$. Given these assumptions, the zeroth-order WTR approximation for canopy drag and the second-order approximation for the effect on the transport of TKE and its dissipation rate become

$$S_U(0) = -C_d a(z)|U|U_i, \qquad (4.5)$$

$$S_k(2) = C_d a(z) \left(-\tfrac{8}{3}|U|k \right), \qquad (4.6)$$

$$S_\varepsilon(2) = C_d a(z) \left(-\tfrac{8}{3}|U|\varepsilon \right); \qquad (4.7)$$

i.e. $\beta_d = 2.67$ and $C_{\varepsilon 5} = 1$.

The zeroth-order approximation for canopy drag (4.5) agrees with the conventional approach (1.1). However, the second-order WTR approximation appears to underestimate the effect on TKE and its dissipation rate when compared with the Silva Lopes *et al.* (2013) reference RANS model (figures 5c and 7c), in which the coefficients ($\beta_d = 4.0$ and $C_{\varepsilon 5} = 0.9$) were calibrated using LES. This is due, in large part, to the effect of the canopy being split into various orders in the WTR approximation, whereas conventional models try to account for it all with a single term, yielding larger coefficients (table 1). Also, the isotropy assumption, although useful in simplifying the equations, is not appropriate inside the canopy. It is sufficient, for instance, to consider the anisotropy commonly found in the Reynolds stresses of homogeneous shear flows, $\overline{u'u'} \approx k$, to obtain $\beta_d = 3.0$ instead of 2.67. In summary, we find that the differences are justified and there is no sign of lack of accuracy in any of the approaches.

5. Summary and conclusions

The canopy-related terms in the transport equations for momentum, TKE and its dissipation rate were approximated using a Taylor series expansion of the velocity magnitude, with a velocity scale based on the total (mean flow and turbulent) kinetic energy. A consistent mathematical formulation was developed in a Reynolds-averaged formulation that, in the case of two-equation (k–ε) turbulence models, implies no additional empirical model coefficients or any uncertainties associated with determining the same. It was shown that in homogeneous canopy flows, the standard RANS formulation is a zeroth-order approximation of momentum and a second-order approximation of both TKE and its dissipation in the WTR formulation.

The conclusions drawn from LES of three canopy flows (over a horizontally homogeneous forest, a sequence of forest stands and clearings, and a forested hill) were as follows:

(i) The limitations inherent in the weak turbulence assumptions (i.e. turbulence intensity much lower than mean velocity or low TKE compared with mean kinetic energy) were overcome by reverting to a velocity scale derived from the total kinetic energy. The model is robust and provided good results, even where these assumptions are questionable, as is the case for non-homogeneous and non-equilibrium flow regions, found near forest edges and on the lee side of forested hills. In the three cases, the perturbative description was valid, leading to a fast-converging series.

(ii) For an accurate representation of the canopy effects in a Reynolds-averaged formulation, momentum in the streamwise direction must be approximated by up to second-order terms.

(iii) The present approach also shows the existence of a drag force perpendicular to the streamwise flow direction. This force, which is about $20\times$ lower than the force along the streamwise direction, must be approximated by second- and third-order terms.

(iv) The TKE requires third-order terms. In the case of the horizontally homogeneous canopy, a 96 % agreement with the LES results was achieved, with the first 84 % being the contributions of the zeroth- and second-order terms.

(v) The modelling of the transport of the TKE dissipation rate was validated under conditions involving only a small fraction of the dissipation being resolved. Nevertheless, a comparison of results obtained with different grid resolutions indicates that the model is also valid and a third-order approximation yields a 100 % agreement with the LES results for the horizontally homogeneous canopy. The series development also shows that the zeroth- and first-order terms are equal to zero, and the second-order term, the lowest approximation of the TKE dissipation rate, yields an accuracy of 84 % in the case of the horizontally homogeneous canopy.

The novelty of this model is that it allows for the determination of canopy effects on the transport of momentum, TKE and its dissipation rate, using a fast-converging series expansion. This, which contrasts with the dimensional arguments used in other turbulence models, may provide the insight required to develop more accurate approaches, thus improving the accuracy of canopy flow prediction in the RANS formulation. We note that although the k–ε model was considered here, the same approach can be applied to second-order Reynolds stress transport models. Results of and assumptions inherent to our model, such as not accounting for TKE wake production and volume fraction, and the uncertainty of both drag coefficient and leaf area index are expected to be minor factors in real life. In such applications, two main difficulties may be encountered: first, our conclusions were based on a comparison of the magnitude of each term of the series with the results of a well-controlled (numerical) experiment, which may differ from laboratory or field measurements; and second, there is the issue of how to translate the higher-order terms of our series into new approximations for canopy-related terms in the RANS formulation, which will depend on the turbulence model being used. These topics are worth addressing in future studies.

Acknowledgements

Declaration of interests

The authors report no conflict of interest.

REFERENCES

ABIVEN, C., PALMA, J. M. L. M. & BRADY, O. 2011 High-frequency field measurements and time-dependent computational modelling for wind turbine siting. *J. Wind Engng Ind. Aerodyn.* **99** (2–3), 123–129.

AYOTTE, K. W., FINNIGAN, J. J. & RAUPACH, M. R. 1999 A second-order closure for neutrally stratified vegetative canopy flows. *Boundary-Layer Meteorol.* **90**, 189–216.

BELCHER, S. E., FINNIGAN, J. J. & HARMAN, I. N. 2008 Flows through forest canopies in complex terrain. *Ecol. Appl.* **18** (6), 1436–1453.

BELCHER, S. E., HARMAN, I. N. & FINNIGAN, J. J. 2012 The wind in the willows: flows in forest canopies in complex terrain. *Annu. Rev. Fluid Mech.* **44** (1), 479–504.

BELCHER, S. E., JERRAM, N. & HUNT, J. C. R. 2003 Adjustment of a turbulent boundary layer to a canopy of roughness elements. *J. Fluid Mech.* **488**, 369–398.

BLACKMAN, K., PERRET, L., CALMET, I. & RIVET, C. 2017 Turbulent kinetic energy budget in the boundary layer developing over an urban-like rough wall using PIV. *Phys. Fluids* **29** (8), 085113-1–085113-19.

BOHRER, G., KATUL, G. G., WALKO, R. L. & AVISSAR, R. 2009 Exploring the effects of microscale structural heterogeneity of forest canopies using large–eddy simulations. *Boundary-Layer Meteorol.* **132** (3), 351–382.

BOU-ZEID, E., OVERNEY, J., ROGERS, B. & PARLANGE, M. 2009 The effects of building representation and clustering in large–eddy simulations of flows in urban canopies. *Boundary-Layer Meteorol.* **132** (3), 415–436.

BOUDREAULT, L.-É., DUPONT, S., BECHMANN, A. & DELLWIK, E. 2017 How forest inhomogeneities affect the edge flow. *Boundary-Layer Meteorol.* **162** (3), 375–400.

BRUNET, Y. 2020 Turbulent flow in plant canopies: historical perspective and overview. *Boundary-Layer Meteorol.* **177** (2), 315–364.

CASTRO, I. P., CHENG, H. & REYNOLDS, R. 2006 Turbulence over urban-type roughness: deductions from wind-tunnel measurements. *Boundary-Layer Meteorol.* **118** (1), 109–131.

CAVA, D. & KATUL, G. G. 2008 Spectral short-circuiting and wake production within the canopy trunk space of an alpine hardwood forest. *Boundary-Layer Meteorol.* **126** (3), 415–431.

CESCATTI, A. & MARCOLLA, B. 2004 Drag coefficient and turbulence intensity in conifer canopies. *Agric. Forest Meteorol.* **121** (3), 197–206.

CHATZIEFSTRATIOU, E. K., VELISSARIOU, V. & BOHRER, G. 2014 Resolving the effects of aperture and volume restriction of the flow by semi-porous barriers using large-eddy simulations. *Boundary-Layer Meteorol.* **152** (3), 329–348.

COSTA, J. C. L., CASTRO, F. A., PALMA, J. M. L. M. & STUART, P. 2006 Computer simulation of atmospheric flows over real forests for wind energy resource evaluation. *J. Wind Engng Ind. Aerodyn.* **94**, 603–620.

DALPÉ, B. & MASSON, C. 2008 Numerical study of fully developed turbulent flow within and above a dense forest. *Wind Energy* **11** (5), 503–515.

DUPONT, S. & BRUNET, Y. 2008 Influence of foliar density profile on canopy flow: a large-eddy simulation study. *Agric. Forest Meteorol.* **148** (6–7), 976–990.

DUPONT, S. & BRUNET, Y. 2009 Coherent structures in canopy edge flow: a large-eddy simulation study. *J. Fluid Mech.* **630**, 93–128.

DUPONT, S., BRUNET, Y. & FINNIGAN, J. J. 2008 Large-eddy simulation of turbulent flow over a forested hill: validation and coherent structure identification. *Q. J. R. Meteorol. Soc.* **134** (636), 1911–1929.

DWYER, M. J., PATTON, E. G. & SHAW, R. H. 1997 Turbulent kinetic energy budgets from a large-eddy simulation of airflow above and within a forest canopy. *Boundary-Layer Meteorol.* **84**, 23–43.

FAO 2012 *Forest Resources Assessment 2015: Terms and Definitions*. Forest Resources Assessment Working Paper – 180 p. 36.

FAO 2016 *Global forest resources assessment 2015: how are the world's forests changing?* OCLC: 1003587002.

FINNIGAN, J. J. 2000 Turbulence in plant canopies. *Annu. Rev. Fluid Mech.* **32**, 519–571.

FINNIGAN, J. J. & SHAW, R. H. 2008 Double-averaging methodology and its application to turbulent flow in and above vegetation canopies. *Acta Geophys.* **56** (3), 534–561.

FOUDHIL, H., BRUNET, Y. & CALTAGIRONE, J.-P. 2005 A fine-scale $k - \varepsilon$ model for atmospheric flow over heterogeneous landscapes. *Environ. Fluid Mech.* **5** (3), 247–265.

GREEN, R. S. 1992 Modelling turbulent air flow in a stand of widely-spaced trees. *Phoenics J.* **5**, 294–312.

KANANI, F., TRÄUMNER, K., RUCK, B. & RAASCH, S. 2014 What determines the differences found in forest edge flow between physical models and atmospheric measurements? An LES study. *Meteorol. Z.* **23** (1), 33–49.

KANDA, M. & HINO, M. 1994 Organized structures in developing turbulent flow within and above a plant canopy, using a large eddy simulation. *Boundary-Layer Meteorol.* **68** (3), 237–257.

KATUL, G. G., MAHRT, L., POGGI, D. & SANZ, C. 2004 One- and two-equation models for canopy turbulence. *Boundary-Layer Meteorol.* **113**, 81–109.

KING, A. T., TINOCO, R. O. & COWEN, E. A. 2012 A k–ε turbulence model based on the scales of vertical shear and stem wakes valid for emergent and submerged vegetated flows. *J. Fluid Mech.* **701**, 1–39.

KOBAYASHI, M. H., PEREIRA, J. C. F. & SIQUEIRA, M. B. B. 1994 Numerical study of the turbulent flow over and in a model forest on a 2D hill. *J. Wind Engng Ind. Aerodyn.* **53**, 357–374.

KRAYENHOFF, E. S., SANTIAGO, J.-L., MARTILLI, A., CHRISTEN, A. & OKE, T. R. 2015 Parametrization of drag and turbulence for urban neighbourhoods with trees. *Boundary-Layer Meteorol.* **156** (2), 157–189.

LIANG, L., XIAOFENG, L., BORONG, L. & YINGXIN, Z. 2006 Improved k-ϵ two-equation turbulence model for canopy flow. *Atmos. Environ.* **40** (4), 762–770.

LIEN, F.-S. & YEE, E. 2004 Numerical modelling of the turbulent flow developing within and over a 3-D building array. Part I: a high-resolution Reynolds-averaged Navier–Stokes approach. *Boundary-Layer Meteorol.* **112** (3), 427–466.

LIEN, F.-S. & YEE, E. 2005 Numerical modelling of the turbulent flow developing within and over a 3-D building array. Part III: a distributed drag force approach, its implementation and application. *Boundary-Layer Meteorol.* **114** (2), 287–313.

LIEN, F.-S., YEE, E. & WILSON, J. D. 2005 Numerical modelling of the turbulent flow developing within and over a 3-D building array. Part II: a mathematical foundation for a distributed drag force approach. *Boundary-Layer Meteorol.* **114** (2), 245–285.

LIU, J., CHEN, J. M., BLACK, T. A. & NOVAK, M. D. 1996 E-ε modelling of turbulent air flow downwind of a model forest edge. *Boundary-Layer Meteorol.* **77** (1), 21–44.

LÓPEZ, F. & GARCÍA, M. H. 2001 Mean flow and turbulence structure of open-channel flow through non-emergent vegetation. *ASCE J. Hydraul. Engng* **127** (5), 392–402.

MARUSIC, I., KUNKEL, G. & PORTÉ-AGEL, F. 2001 Experimental study of wall boundary conditions for large-eddy simulation. *J. Fluid Mech.* **446**, 309–320.

MASON, P. J. & THOMSON, D. J. 1992 Stochastic backscatter in large-eddy simulations of boundary layers. *J. Fluid Mech.* **242**, 51–78.

MENEVEAU, C., LUND, T. S. & CABOT, W. H. 1996 A Lagrangian dynamic subgrid-scale model of turbulence. *J. Fluid Mech.* **319**, 353–385.

MEYERS, T. P. & BALDOCCHI, D. D. 1991 The budgets of turbulent kinetic energy and Reynolds stress within and above a deciduous forest. *Agric. Forest Meteorol.* **53** (3), 207–222.

MOCHIDA, A., TABATA, Y., IWATA, T. & YOSHINO, H. 2008 Examining tree canopy models for CFD prediction of wind environment at pedestrian level. *J. Wind Engng Ind. Aerodyn.* **96** (10–11), 1667–1677.

NEARY, V. S. 2003 Numerical solution of fully developed flow with vegetative resistance. *J. Engng Mech. ASCE* **129** (5), 558–563.

NEBENFÜHR, B. & DAVIDSON, L. 2015 Large-eddy simulation study of thermally stratified canopy flow. *Boundary-Layer Meteorol.* **156** (2), 253–276.

NOVAK, M. D., WARLAND, J. S., ORCHANSKY, A. L., KETLER, R. & GREEN, S. 2000 Wind tunnel and field measurements of turbulent flow in forests. Part I: uniformly thinned stands. *Boundary-Layer Meteorol.* **95**, 457–495.

PAN, Y., BIRDSEY, R. A., PHILLIPS, O. L. & JACKSON, R. B. 2013 The structure, distribution, and biomass of the world's forests. *Annu. Rev. Ecol. Evol. Syst.* **44** (1), 593–622.

PATTON, E. G., HORST, T. W., SULLIVAN, P. P., LENSCHOW, D. H., ONCLEY, S. P., BROWN, W. O. J., BURNS, S. P., GUENTHER, A. B., HELD, A., KARL, T., *et al.* 2011 The canopy horizontal array turbulence study. *Bull. Am. Meteorol. Soc.* **92** (5), 593–611.

PATTON, E. G., SHAW, R. H., JUDD, M. J. & RAUPACH, M. R. 1998 Large-eddy simulations of windbreak flow. *Boundary-Layer Meteorol.* **87**, 275–306.

PINARD, J. D. J.-P. & WILSON, J. D. 2001 First- and second-order closure models for wind in a plant canopy. *J. Appl. Meteorol.* **40**, 1762–1768.

POGGI, D., KATUL, G. G. & VIDAKOVIC, B. 2011 The role of wake production on the scaling laws of scalar concentration fluctuation spectra inside dense canopies. *Boundary-Layer Meteorol.* **139** (1), 83–95.

RAUPACH, M. R. & SHAW, R. H. 1982 Averaging procedures for flow within vegetation canopies. *Boundary-Layer Meteorol.* **22** (1), 79–90.

RAUPACH, M. R. & THOM, A. S. 1981 Turbulence in and above plant canopies. *Annu. Rev. Fluid Mech.* **13**, 97–129.

RAUPACH, M. R., THOM, A. S. & EDWARDS, I. 1980 A wind-tunnel study of turbulent flow close to regularly arrayed rough surfaces. *Boundary-Layer Meteorol.* **18** (4), 373–397.

ROSENFELD, M., MAROM, G. & BITAN, A. 2010 Numerical simulation of the airflow across trees in a windbreak. *Boundary-Layer Meteorol.* **135** (1), 89–107.

SAGAUT, P. 2006 *Large eddy simulation for incompressible flows: an introduction*, 3rd edn. Scientific Computation Springer.

SANZ, C. 2003 A note on $k - \varepsilon$ modelling of vegetation canopy air-flows. *Boundary-Layer Meteorol.* **108** (1), 191–197.

SANZ, C. & KATUL, G. G. 2007 Dual length scale two-equation modelling of the canopy turbulent kinetic energy wake budget. *C. R. Méc.* **335** (11), 685–690.

SCHLEGEL, F., STILLER, J., BIENERT, A., MAAS, H.-G., QUECK, R. & BERNHOFER, C. 2015 Large-eddy simulation study of the effects on flow of a heterogeneous forest at sub-tree resolution. *Boundary-Layer Meteorol.* **154** (1), 27–56.

SCHROTTLE, J. & DORNBRACK, A. 2013 Turbulence structure in a diabatically heated forest canopy composed of fractal Pythagoras trees. *Theor. Comput. Fluid Dyn.* **27** (3–4), 337–359.

SHAW, R. H. & PATTON, E. G. 2003 Canopy element influences on resolved- and subgrid-scale energy within a large-eddy simulation. *Agric. Forest Meteorol.* **115** (1–2), 5–17.

SHAW, R. H. & SCHUMANN, U. 1992 Large-eddy simulation of turbulent flow above and within a forest. *Boundary-Layer Meteorol.* **61**, 47–64.

SHEN, S. & LECLERC, M. Y. 1997 Modelling the turbulence structure in the canopy layer. *Agric. Forest Meteorol.* **87** (1), 3–25.

SILVA LOPES, A., PALMA, J. M. L. M. & CASTRO, F. A. 2007 Simulation of the Askervein flow. Part 2: large-eddy simulations. *Boundary-Layer Meteorol.* **125** (1), 85–108.

SILVA LOPES, A., PALMA, J. M. L. M. & PIOMELLI, U. 2015 On the determination of effective aerodynamic roughness of surfaces with vegetation patches. *Boundary-Layer Meteorol.* **156** (1), 113–130.

SILVA LOPES, A., PALMA, J. M. L. M. & VIANA LOPES, J. 2013 Improving a two-equation turbulence model for canopy flows using large-eddy simulation. *Boundary-Layer Meteorol.* **149** (2), 231–257.

SILVA LOPES, A., PALMA, J. M. L. M. & VIANA LOPES, J. 2016 Modelling flows within forested areas using the $k - \varepsilon$ RaNS model. *J. Phys.: Conf. Ser.* **753** (8), 082035.

SOGACHEV, A. 2009 A note on two-equation closure modelling of canopy flow. *Boundary-Layer Meteorol.* **130** (3), 423–435.

SOGACHEV, A., KELLY, M. & LECLERC, M. Y. 2012 Consistent two-equation closure modelling for atmospheric research: buoyancy and vegetation implementations. *Boundary-Layer Meteorol.* **145** (2), 307–327.

SOGACHEV, A., MENZHULIN, G. V., HEIMANN, M. & LLOYD, J. 2002 A simple three-dimensional canopy – planetary boundary layer simulation model for scalar concentrations and fluxes. *Tellus B* **54** (5), 784–819.

SOGACHEV, A. & PANFEROV, O. 2006 Modification of two-equation models to account for plant drag. *Boundary-Layer Meteorol.* **121** (2), 229–266.

Su, H.-B., Shaw, R. H., Paw U, K. T., Moeng, C.-H. & Sullivan, P. P. 1998 Turbulent statistics of neutrally stratified flow within and above a sparse forest from large–eddy simulation and field observations. *Boundary-Layer Meteorol.* **88**, 363–397.

Svensson, U. & Häggkvist, K. 1990 A two-equation turbulence model for canopy flows. *J. Wind Engng Ind. Aerodyn.* **35**, 201–211.

Wilson, J. D. 1988 A second-order closure model for flow through vegetation. *Boundary-Layer Meteorol.* **42** (4), 371–392.

Wilson, J. D., Finnigan, J. J. & Raupach, M. R. 1998 A first-order closure for disturbed plant-canopy flows, and its application to winds in a canopy on a ridge. *Q. J. R. Meteorol. Soc.* **124** (547), 705–732.

Wilson, N. R. & Shaw, R. H. 1977 A higher order closure model for canopy flow. *J. Appl. Meteorol.* **16** (11), 1197–1205.

Yamada, T. 1982 A numerical model study of turbulent airflow in and above a forest canopy. *J. Meteorol. Soc. Japan* **60** (1), 439–454.

Yan, C., Huang, W.-X., Miao, S.-G., Cui, G.-X. & Zhang, Z.-S. 2017 Large-eddy simulation of flow over a vegetation-like canopy modelled as arrays of bluff-body elements. *Boundary-Layer Meteorol.* **165** (2), 233–249.

Yang, B., Morse, A. P., Shaw, R. H. & Paw U, K. T. 2006 Large-eddy simulation of turbulent flow across a forest edge. Part II: momentum and turbulent kinetic energy budgets. *Boundary-Layer Meteorol.* **121** (3), 433–457.

Yue, W., Meneveau, C., Parlange, M. B., Zhu, W., Kang, H. S. & Katz, J. 2008 Turbulent kinetic energy budgets in a model canopy: comparisons between LES and wind-tunnel experiments. *Environ. Fluid Mech.* **8** (1), 73–95.

Yue, W., Parlange, M., Meneveau, C., Zhu, W., van Hout, R. & Katz, J. 2007 Large-eddy simulation of plant canopy flows using plant-scale representation. *Boundary-Layer Meteorol.* **124** (2), 183–203.